SUPPLEMENTARY INFORMATION AND METHODS FOR

Protocol for Performing and Optimizing Differential Scanning Fluorimetry Experiments

Taiasean Wu, Michael Hornsby, Lawrence Zhu, Joshua C. Yu, Kevan M. Shokat, and Jason E. Gestwicki

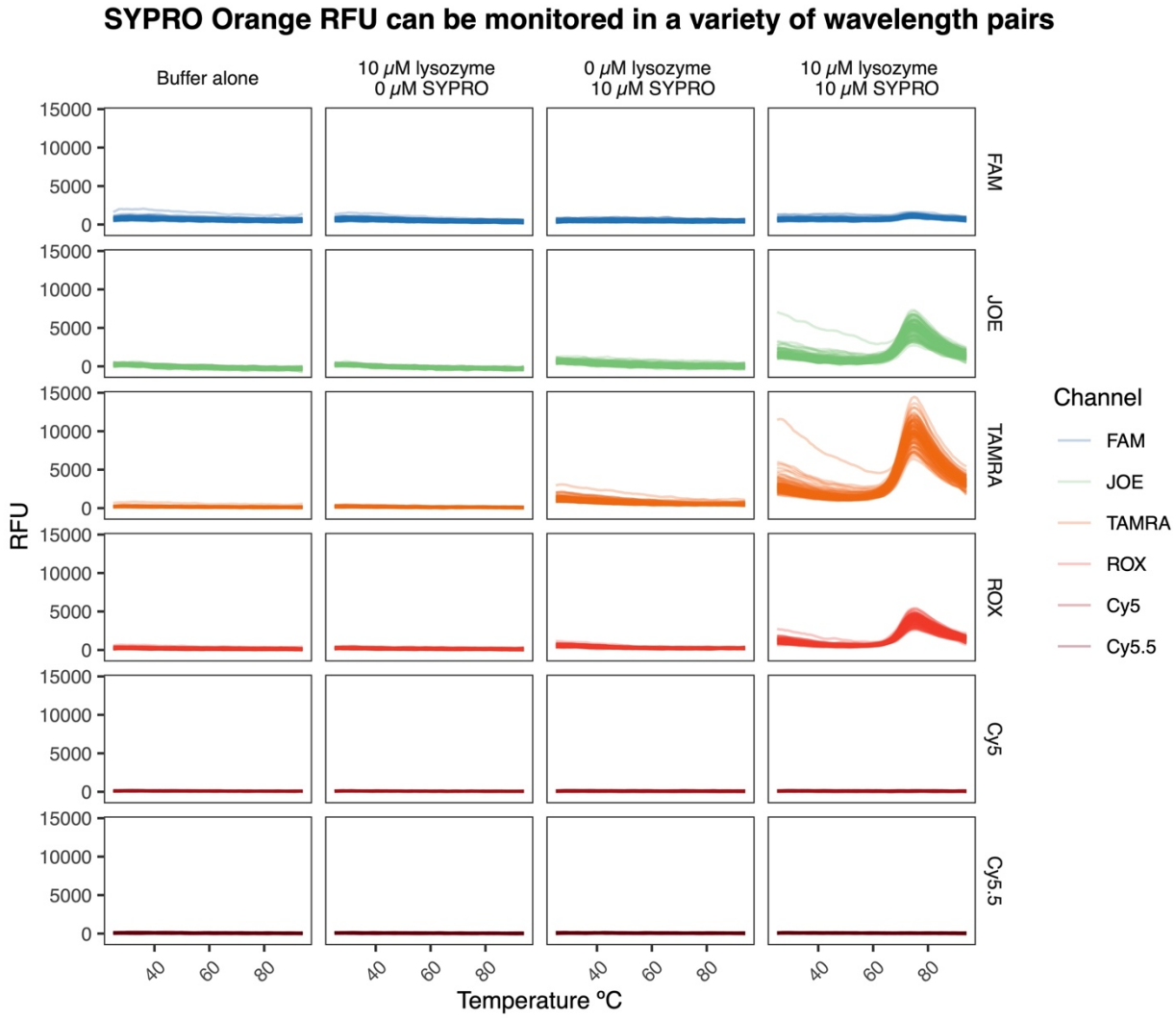

Figure S1. SYPRO Orange RFU can be monitored with a wide variety of channels. Beyond the typical channels for SYPRO Orange measurement (e.g. "FRET" (~485/605 nm), SYPRO Orange fluorescence for DSF can be monitored in a wide range of additional channels, including JOE (515/5454 nm), TAMRA (535/580 nm), and ROX (565/605).

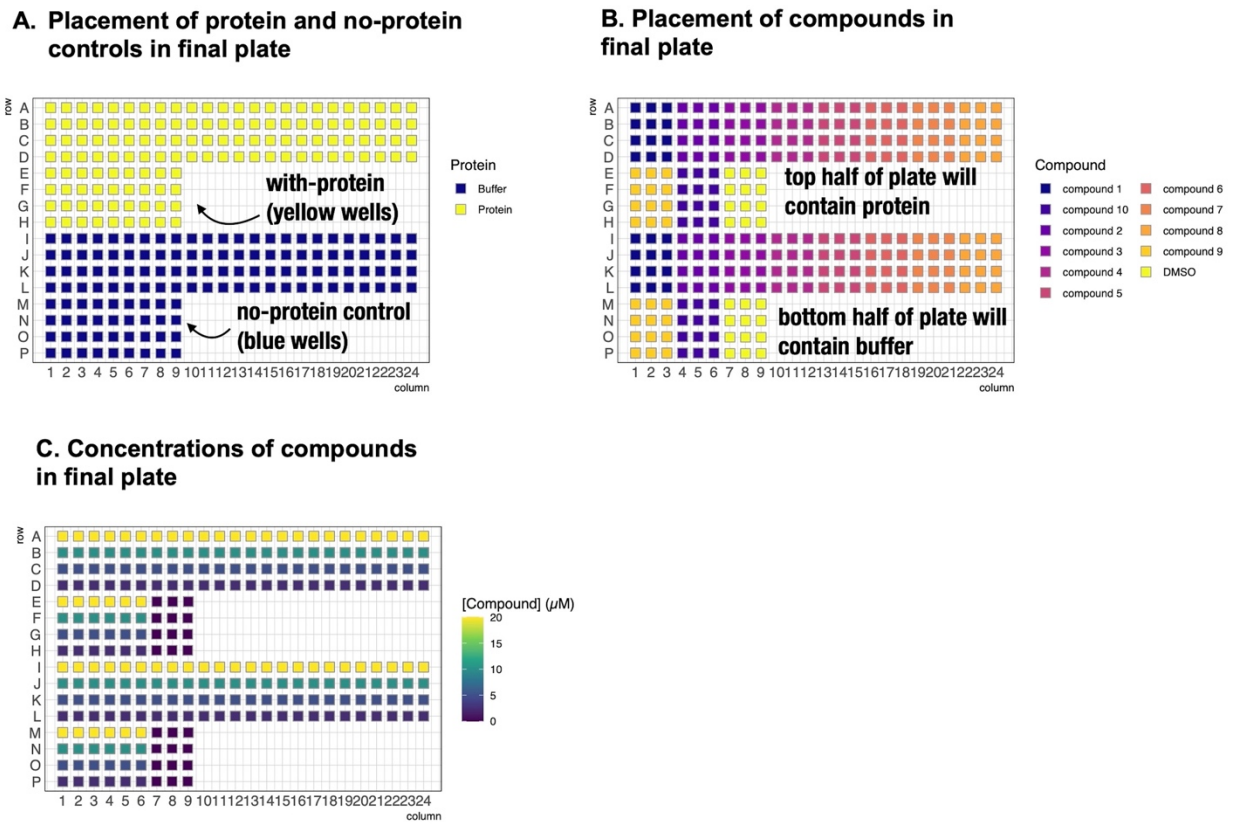

Figure S2. Plate-view maps of the final 10-compound DSF experiment described in the Step-by-step protocol. The three key variables in the final experiment are presented in panels A-C above. A. The placement of protein or buffer in the plate. Only half of the wells in the experiment contain protein, because a no-protein control is included for each tested condition. B. The placement of compounds in the final plate. All compounds are tested in triplicate. Note that the with-protein and no-protein regions of the plate (see panel A) contain identical compounds.C. The concentrations of the compounds in the plate. Note that all compounds are tested at four different concentrations, with both protein and no-protein controls.

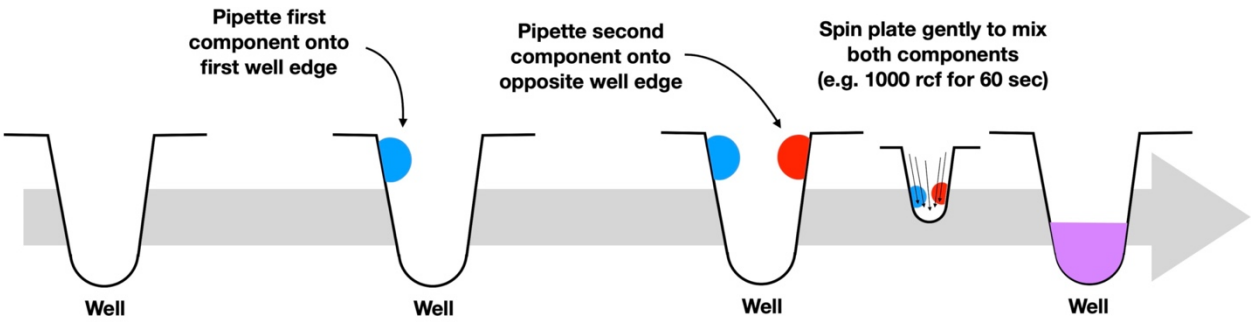

Figure S3. Pipetting small volumes onto top-edges of wells can make it easier to set up large, complex experiments in well plates. The pipetted droplets are settled into the bottoms of the wells and mixed by centrifuging the plate prior to incubation and placement in the qPCR.

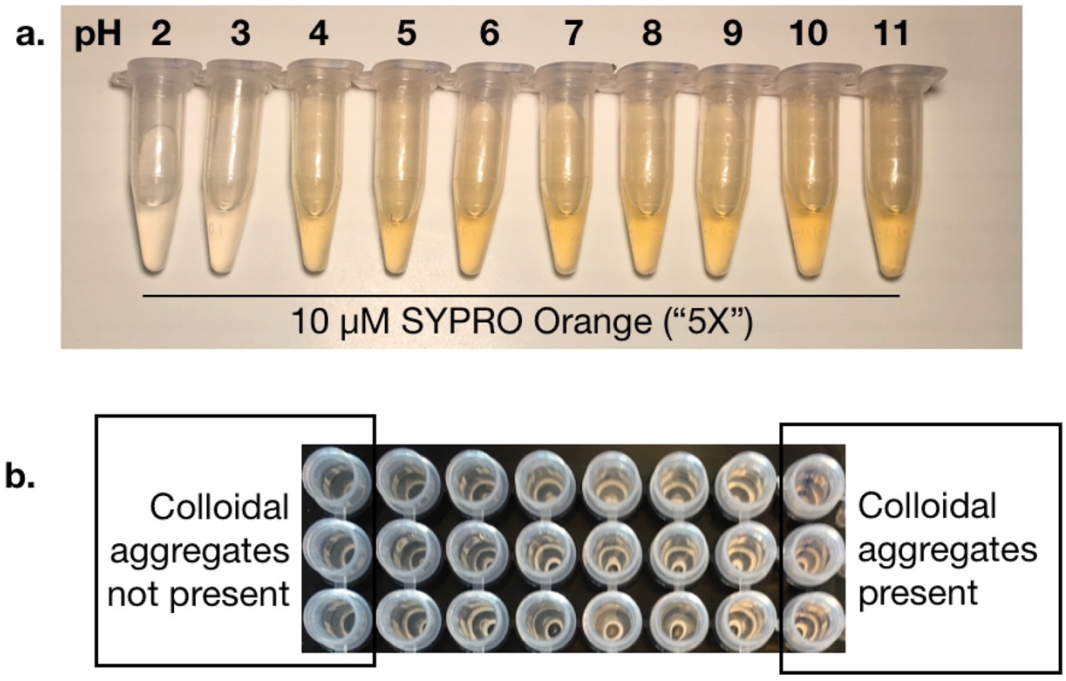

Figure S4. Changes in visual pigmentation of 10 µM ("5X") SYPRO Orange solutions with pH or small molecule colloidal aggregation. Changes in visual pigmentation of 10 µM ("5X") SYPRO Orange solutions with pH or small molecule colloidal aggregation. a. 10 µM solutions of SYPRO Orange, displaying decreased room temperature pigmentation in low-pH PBS. b. 10 µM solutions of SYPRO Orange, displaying increased room temperature pigmentation in the presence of small molecule colloidal aggregates. The presence of colloidal aggregates was determined by DLS; see figures S5—S7

	Drug name	Citation	Typical use	Vendor	Catalog #	SMILES
1	Vemurafenib	1	anti-neoplastic melanoma	Cell Signaling Technology, Inc.	17531S	ClC1=CC=C(C2=CN=C(NC=C3C(C4=C(F)C=CC(NS(CCC)(=O)=O)=C4F)=O)C3=C2)C=C1
2	Miconazole	1	anti-fungal	Emolecules Inc	501598605	ClC1=CC=C(COC(C2=C(Cl)C=C(Cl)C=C2)CN3C=CN=C3)C(Cl)=C1
3	Clotrimazole	1	anti-fungal	Emolecules Inc	501544319	ClC(C=CC=C1)=C1C(C2=CC=CC=C2)(N3C=NC=C3)C4=CC=CC=C4
4	Ritonavir	1	anti-retroviral	Adipogen Corporation	501687445	O=C(NC(C(CC(NC(C(NC(N(CC1=CSC(C(C)C)=N1)C)=O)C(C)C)=O)CC2=CC=CC=C2)O)CC3=CC=CC=C3)OCC4=CN=CS4
5	Emodin	1	natural product	Selleck Chemical Llc	501362252	OC1=C2C(C(C(C=C(O)C=C3O)=C3C2=O)=O)=CC(C)=C1
6	Crizontinib	2	anti-non small cell lung carcinoma	Medchemexpress Llc	501873893	CC(C1=C(Cl)C=CC(F)=C1Cl)OC2=C(N)C=CC(C(C=N3)=CN3C4CCNCC4)=C2
7	Sorafenib	2	advanced renal cell carcinoma	Medchemexpress Llc	501871951	CNC(C1=NC=CC(OC2=CC=C(NC(NC3=CC(C(F)(F)F)=C(Cl)C=C3)=O)C=C2)=C1)=O
8	Danazol	1	endometriosis	SIGMA-ALDRICH	D8399-100MG	CC1(C2)C(CCC3C1CCC4C3CCC4(O)C#C)=CC5=C2C=CO5
						ClC1=CC=C(C2=CN=C(NC=C3C(C4=C(F)C=CC(NS(CCC)(=O)=O)=C4F)=O)C3=C2)C=C1

Table S1. Diversified functions and commercial sources of the panel of compounds used for colloidal aggregation experiments. Compounds assembled from Ganesh et al [1] and Owen et al [2].

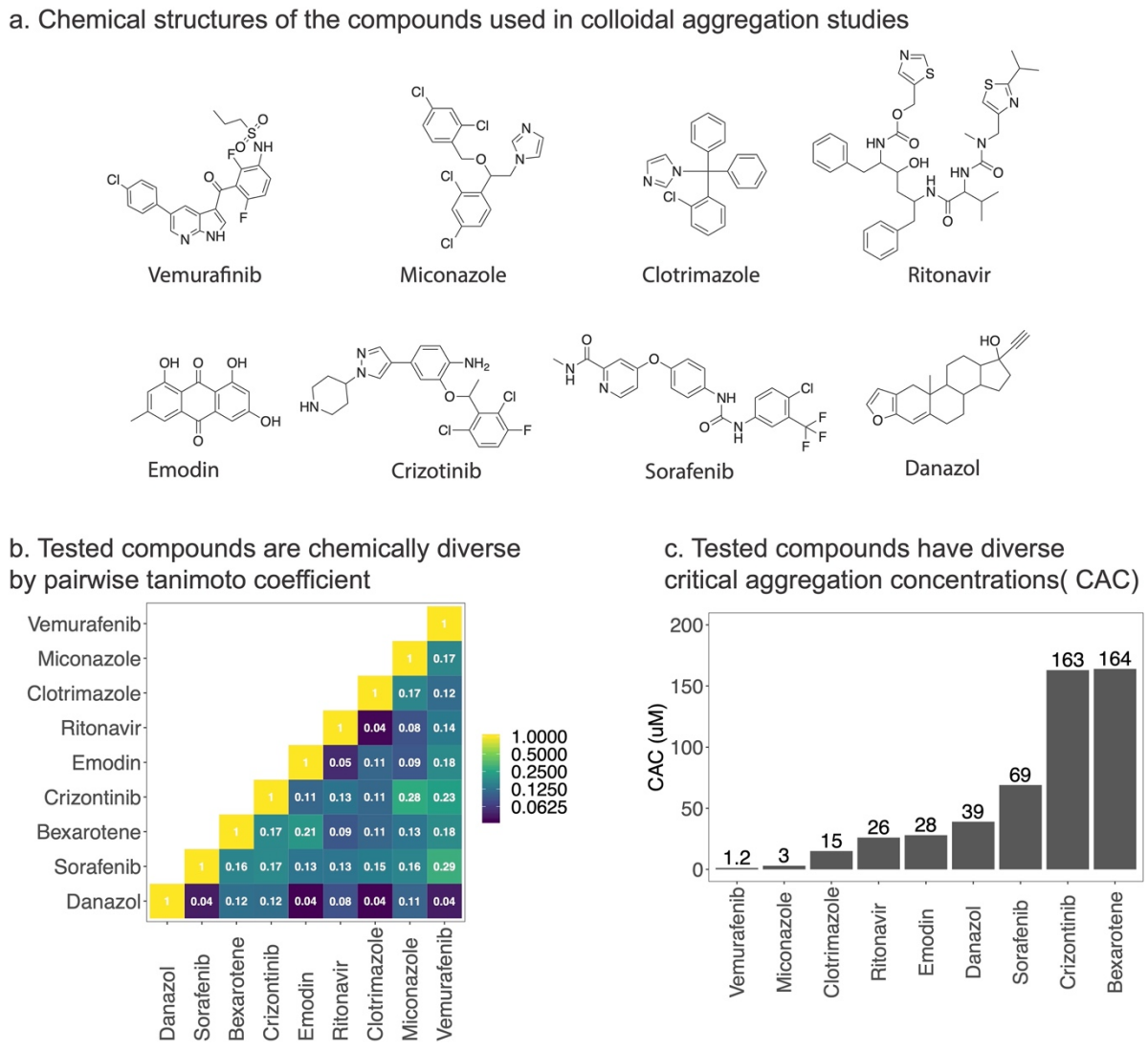

Figure S5. Properties of the compounds used for colloidal aggregation experiments. a. Chemical structures of the eight compounds in the panel. b. The compounds are structurally and chemically diverse, as described by low pair-wise AP tanimoto score coefficients, calculated by chemmineR package and online tools (https://chemminetools.ucr.edu/about/). c. The compounds cover a large range of critical aggregation concentration (CAC) values; values taken from Ganesh et al [1] and Owen et al [2].

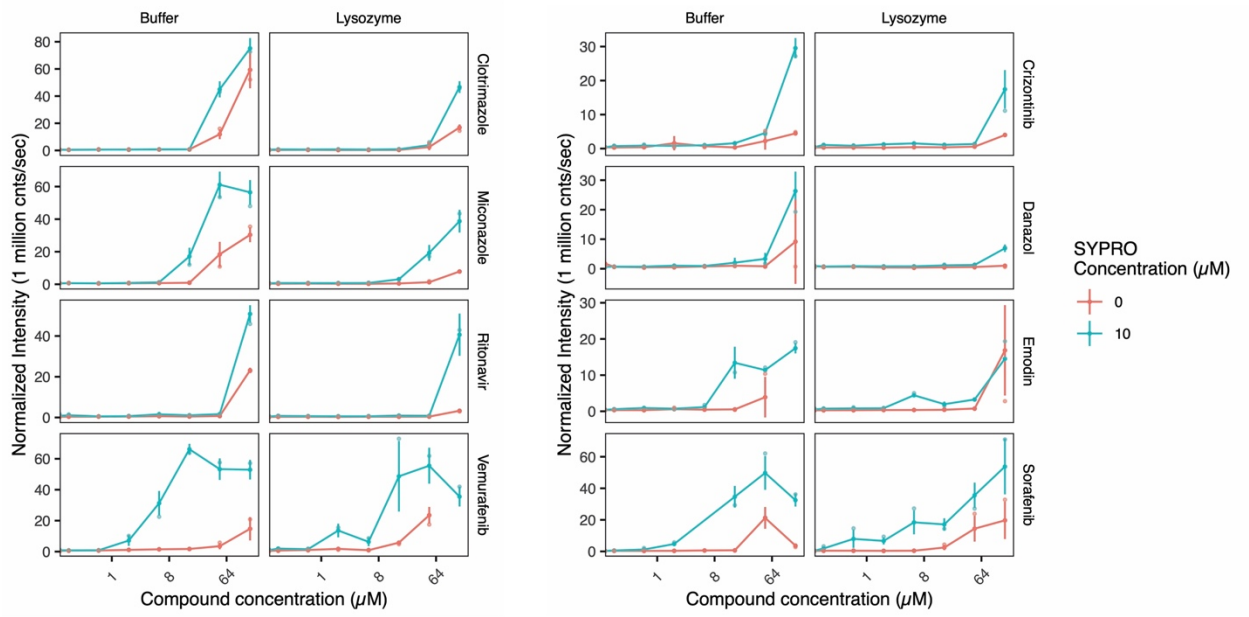

Figure S6. Colloidal aggregation of small molecules as measured by DLS. Dynamic Light Scattering (DLS) of the eight small molecules in the absence and presence of SYPRO Orange and 1 µM lysozyme. All eight compounds (Clotrimazole, Miconazole, Vemurafenib, Crizotinib, Danazol, Emodin, Sorafenib) form colloidal aggregates within the tested concentrations (0 - 150 µM) for all conditions as determined by Dynamic Light Scattering (DLS) in buffer (10 mM HEPES, 200 mM NaCl, pH 7.20, 0.22 µm filtered). In all cases, the presence of 5X SYPRO Orange (teal lines) increased aggregation, while the addition of 1 µM lysozyme reduced it. For SYPRO Orange, "5X" corresponds to ~10 µM, see Figures S8 and S9.

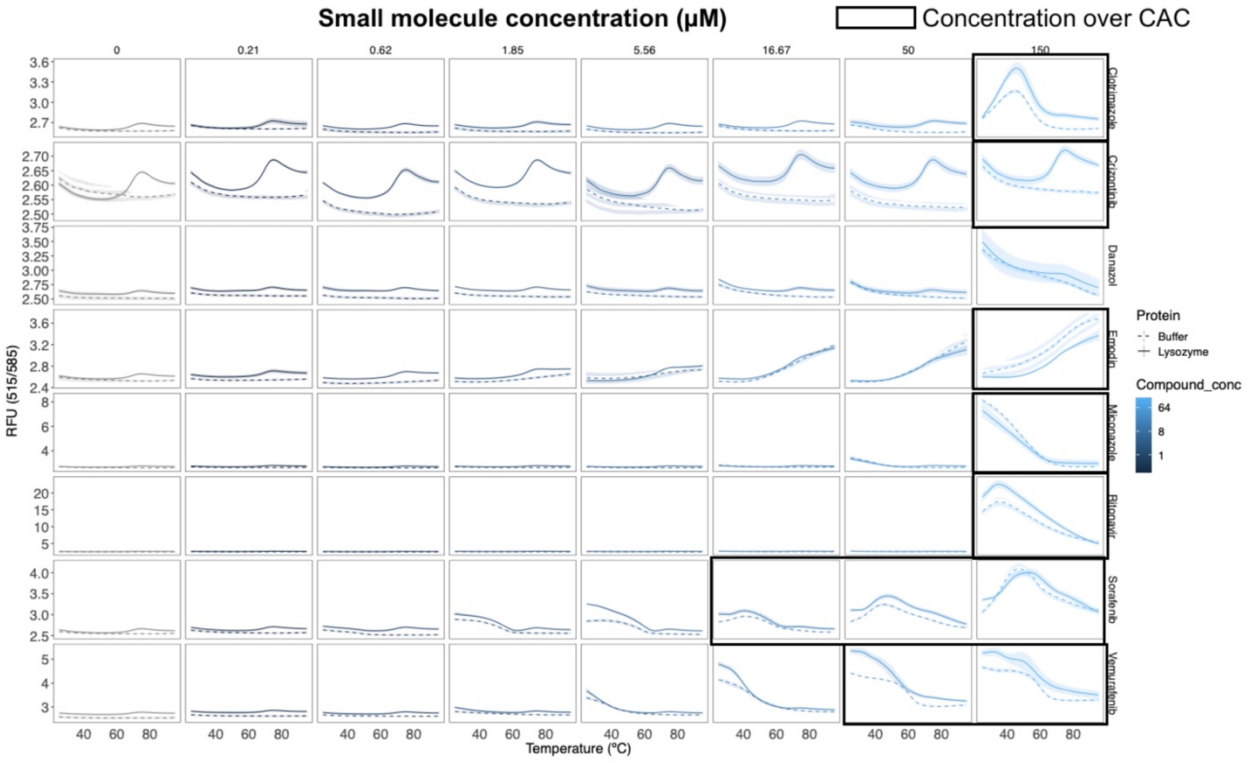

Figure S7. Influence of small molecules on protein-independent fluorescence correlates to colloidal aggregate abundance. Colloidal aggregates interfere with DSF signal, independent of protein. At concentrations above the CAC, aberrant dye fluorescence is observed by DSF in the presence of buffer, dye, and compound alone (dotted lines). The aberrations are sufficient to obscure the melting signal of 1µM lysozyme (solid lines).

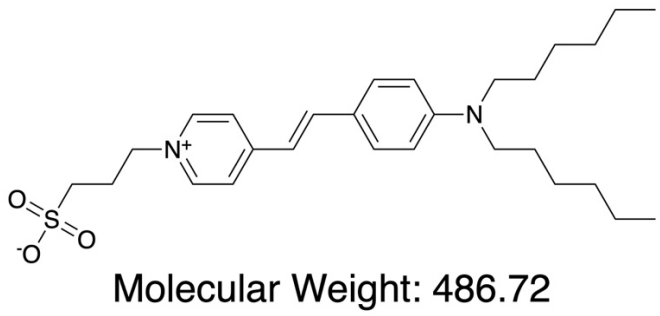

Molecular Weight: 486.72

Figure S8. The structure of commercial SYPRO Orange. LCMS (m/z) calculated 486.29, observed 487.0. This structure is consistent with that reported by Kroger et. al.[3] Using the molecular weight of 486.29 g/mol for SYPRO Orange, the concentration of the 5000X stock was calculated to be 10.4 +/- 0.2 mM.

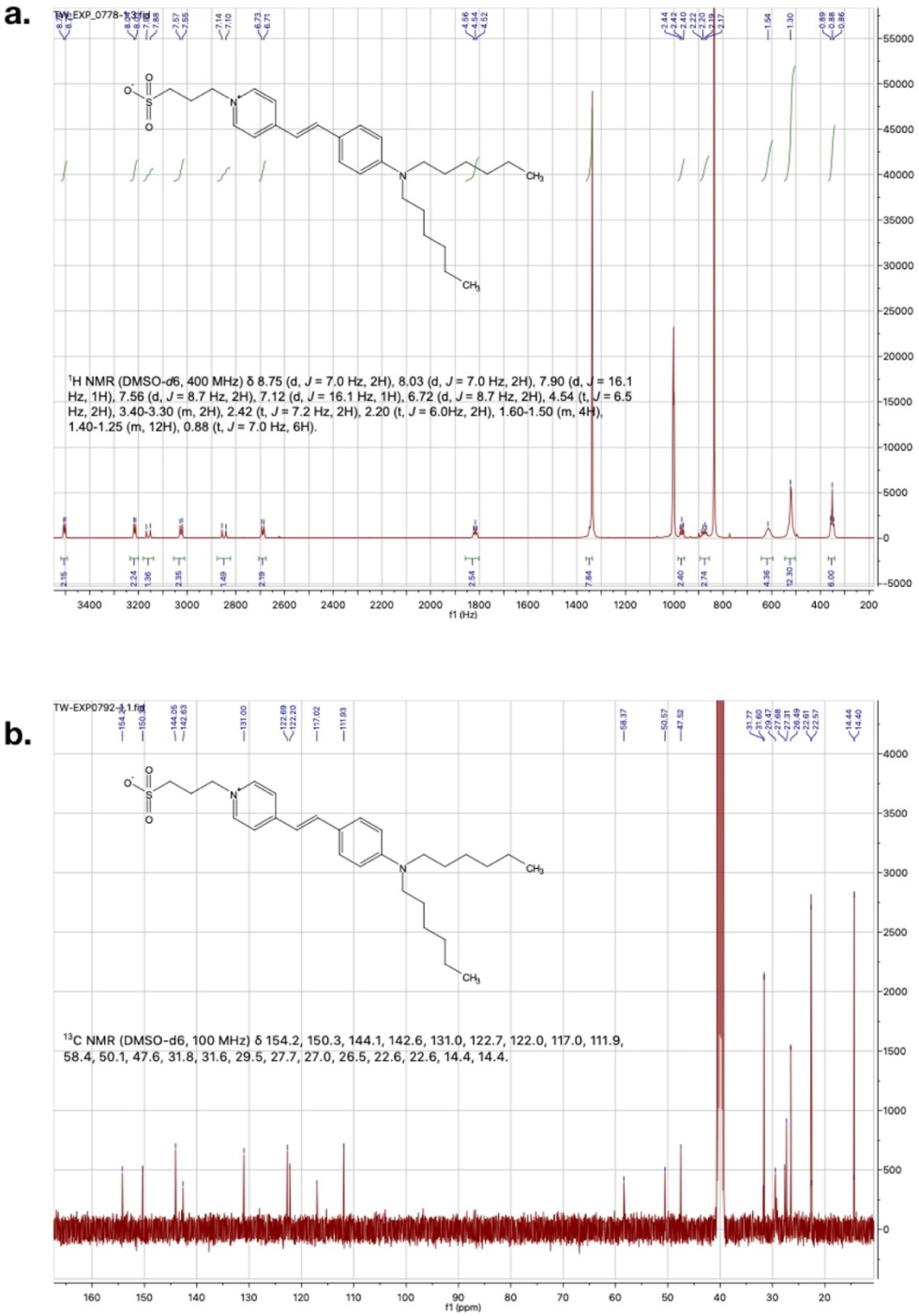

Figure S9. Characterization of commercial SYPRO Orange. The structure of commercial SYPRO Orange was determined by 1H-NMR and 13C-NMR. The molecular mass was confirmed by LCMS (m/z) calculated 486.29, observed 487.0. a. 1H-NMR of commercial SYPRO Orange. (DMSO-d6, 400 MHz) δ 8.75 (d, J = 7.0 Hz, 2H), 8.03 (d, J = 7.0 Hz, 2H), 7.90 (d, J = 16.1 Hz, 1H), 7.56 (d, J = 8.7 Hz, 2H), 7.12 (d, J = 16.1 Hz, 1H), 6.72 (d, J = 8.7 Hz, 2H), 4.54 (t, J = 6.5 Hz, 2H), 3.40-3.30 (m, 2H), 2.42 (t, J = 7.2 Hz, 2H), 2.20 (t, J = 6.0Hz, 2H), 1.60-1.50 (m, 4H), 1.40-1.25 (m, 12H), 0.88 (t, J = 7.0 Hz, 6H). b. 13C-NMR of commercial SYPRO Orange. (DMSO-d6, 100 MHz) δ 154.2, 150.3, 144.1, 142.6, 131.0, 122.7, 122.0, 117.0, 111.9, 58.4, 50.1, 47.6, 31.8, 31.6, 29.5, 27.7, 27.0, 26.5, 22.6, 22.6, 14.4, 14.4.

Protein	MW (kDa)	Experimental purpose	Function	Published oligomeric state
Lysozyme	14.3	Benchmark of reversible (equilibrium)	Lysosomal hydrolase	Monomer
Malate dehydrogenase (MDH)	36.2	Benchmark of irreversible (kinetic) unfolding in Figure 1	Periportal/ oxidative enzyme	Dimer
PPIF	22.04	Test case	Cyclophilin	Monomer
PPIE	42	Test case	Metabolic enzyme	Decamer
PerAB Early Doors Mutant	38.632	Test case	Circadian-regulator, clock-shift mutant	Dimer
Per2	38.632	Test case	Circadian regulator	Dimer
Hsc70	70.898	Test case	Molecular chaperone	Monomer
CHIP	32.69	Test case	E3 ligase	Dimer

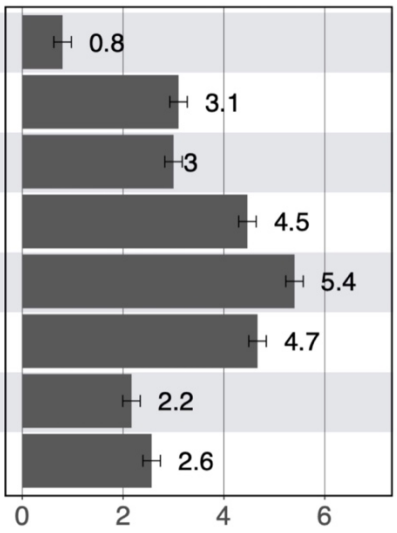

Table S2. Properties of the proteins tested for the effects of heating rate. Details on the representative protein panel from Figure 1, which were selected to sample different sizes, function, and oligomeric states. The range of Tma values ΔTma determined at four heating rates (0.25, 0.5, 1 and 2 ºC/min) is also shown. The error bars represent standard deviation from at least two independent experiments.

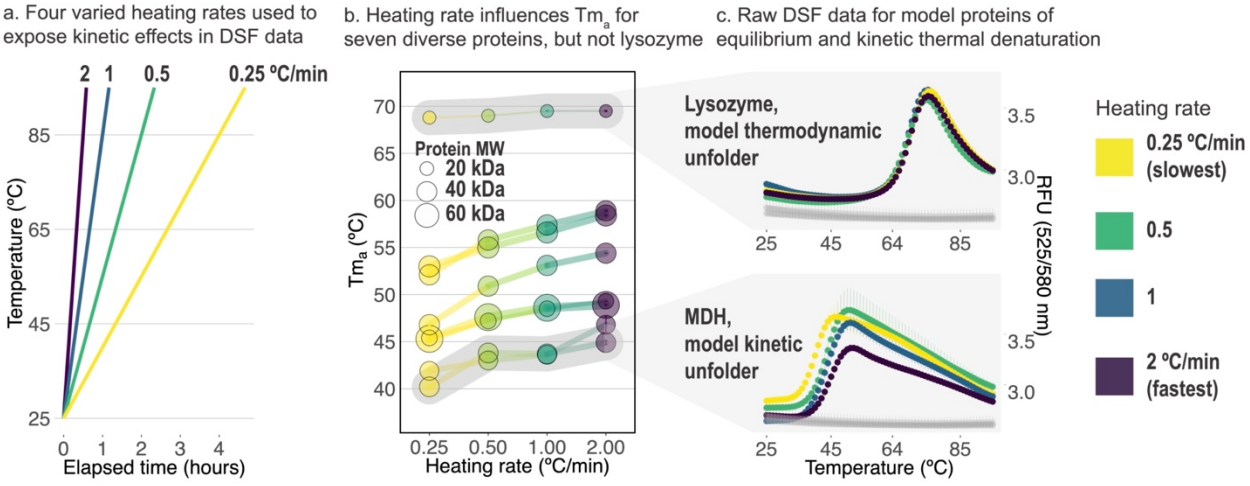

Figure S10. The kinetics of protein unfolding impact DSF results. a. Schematic of the four thermocycling protocols used to generate results presented in b, highlighting the different elapsed times required to reach the same temperature between them. b. From the diverse eight protein panel, seven display heating-rate dependent changes in Tma, similar to the model irreversible unfolder malate dehydrogenase (MDH). Only the model reversible unfolder lysozyme shows heating rate-independent Tmas. c. Raw DSF data for model equilibrium unfolding protein lysozyme and model kinetic unfolding protein MDH at the four ramp rates. No-protein controls (5X SYPRO Orange in buffer) are shown in grey. Results presented are the average of from three technical replicates +/- standard deviation.

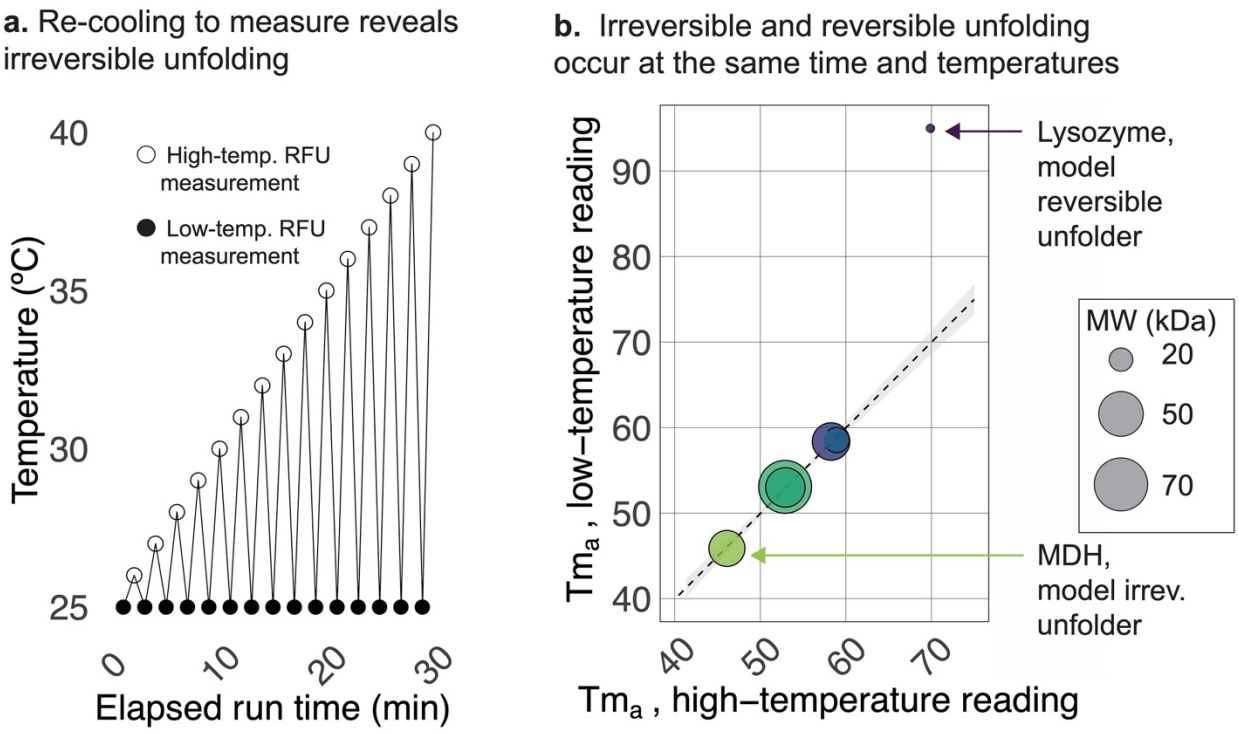

Figure S11. Irreversible and reversible unfolding take place at the same temperatures for a diverse panel of proteins. a. Schematic of the "up-down mode" thermocycling protocol used to emphasize the contribution of irreversible unfolding in a DSF experiment. Briefly, the irreversible state is maintained at low temperature, while the high temperature samples both reversible and irreversible unfolding. b. Tma values produced from DSF experiments performed at either high-temperatures (reversible and irreversible) or low-temperatures (irreversible only) agree for all proteins except the model reversible-unfolding protein lysozyme, as expected. This result suggests that the temperature at which irreversible unfolding is significant (precisely, k = 1/min) is likely near or equal to the thermodynamic melting temperature $T_{1/2}$).

Methods S1. Methods corresponding to results in the supplementary information.

Processing of ProTherm Data.

The full ProTherm dataset (ProTherm.dat) was downloaded from GitHub (https://github.com/protabit/protherm-conversion). Unique proteins were defined as those which had distinct values for both the protein name (PROTEIN) and organism (SOURCE). For the proteins for which multiple Tm_as were available, we calculated the average. Differences in Tm_a (ΔTm_a) that are due to mutations were calculated by subtracting the value from wild type. Likewise, ΔTm_a from changes in buffer were determined by comparing the individual effects of changing concentration, salt or pH.

Analyses of SYPRO Orange.

From 200 µL of 5000X SYPRO Orange stock (Thermo Fisher Scientific Reference S6650, Lot 2008138), a dry red powder was produced by removal of DMSO under reduced pressure in the dark (GeneVac EZ-2 Elite, High BP setting, lamp off). Presented results are from six technical replicates over two separate experiments. LC-MS spectra were collected on an Agilent ACQ-TQD in 0.1% Formic Acid; NMR spectra were collected in d6-DMSO on a Bruker (400 MHz ^{1}H/100 MHz ^{13}C).

Differential Scanning Fluorimetry.
Unless otherwise noted, conditions for all DSF experiments presented in the Troubleshooting section were: 10 µM protein; 10 µM ("5X") SYPRO Orange, (Thermo Fisher Scientific Ref S6650, Lot 2008138) in 10 mM HEPES, 200 mM NaCl, pH 7.2, 0.22 µm filtered (Millex-GS 0.22 µm sterile filter unit, ref SLGS033ss, lot R8EA61590), with a final DMSO concentration of 0.1% and final reaction volume 10 µL per well in a 384-well microtiter plate (Axygen PCR-284-LC480WNFBC Lot 09819000). DSF experiments were monitored in a BioRad CFX 384 qPCR in the FRET channel.

Dynamic Light Scattering.
From 5 mM stocks in DMSO (Sigma Aldrich prod 276855-100 mL lot SHBK3913), six 3-fold serial dilutions of each compound were prepared in DMSO (150 – 0.2 µM), diluted in 10 mM HEPES, 200 mM NaCl, pH 7.20, and combined with either buffer or lysozyme, with or without SYPRO Orange, to final concentrations of 10 µM lysozyme, 150 – 0.20 µM compound, 10 µM SYPRO Orange, 2.5% DMSO. All reagents were filtered prior to use (Millex-GS 0.22 µm sterile filter unit, ref SLGS033ss, lot R8EA61590). 20 µL of each final solution was added to a DLS plate with no plate seal, and colloidal aggregation was measured using a Wyatt Technologies DynaPro Plate Reader II (acquisition time 2 sec, 20 acquisitions, with auto-attenuation, with temperature control, 25 °C). For the matched DSF experiments, 10 µL of the same solutions was added to each well of a DSF plate (Axygen PCR-284-LC480WNFBC Lot 09819000) and heated from 25 – 95 °C at a heating rate of 1 °C/min and monitored in the FRET channel of a BioRad CFX384. Experiments were performed in technical triplicate and presented as mean +/- standard deviation.

Glycerol viscosity.
5000X SYPRO Orange was diluted to 10 µM ("5X") in each glycerol:ddH2O mixtures (mol/mol; Sigma-Aldrich G7893-2L) and mixed thoroughly. Then, 40 µL of each mixture was added to each well of a clear, flat-bottom 384-well plate (Greiner Bio-One ref 781091). Solutions were photo-graphed in ambient daylight. On a Molecular Devices Spectra-Max M5 fitted with a 384-well plate adaptor, absorbance spectra was measured from 350 – 700 nm. Emission following excitation at 485 nm was collected every 10 nm from 515 nm to 750 nm.

Supplementary references.

1. Ganesh, A.N., Donders, E.N., Shoichet, B.K., and Shoichet, M.S. (2018). Colloidal aggregation: From screening nuisance to formulation nuance. Nano Today *19*, 188–200.

2. Owen, S.C., Doak, A.K., Wassam, P., Shoichet, M.S., and Shoichet, B.K. (2012). Colloidal aggregation affects the efficacy of anticancer drugs in cell culture. ACS Chem. Biol. *7*, 1429–1435.

3. Kroeger, T., Frieg, B., Zhang, T., Hansen, F.K., Marmann, A., Proksch, P., Nagel-Steger, L., Groth, G., Smits, S.H.J., and Gohlke, H. (2017). EDTA aggregates induce SYPRO orange-based fluorescence in thermal shift assay. PLoS One *12*, e0177024.